Catalysis Today 430 (2024) 114515

Contents lists available at ScienceDirect

Catalysis Today

journal homepage: www.elsevier.com/locate/cattod

Amino-grafted basic mesoporous silicas: a type of highly performant catalysts for the green synthesis of 2-amino-4*H*-chromenes

Daniel González-Rodal [a], Marina Godino-Ojer [a], Carlos Palomino-Cabello [b], Gemma Turnes-Palomino [b,*], Antonio J. López-Peinado [c], Elena Pérez-Mayoral [c,*]

[a] *Facultad de Ciencias Experimentales, Universidad Francisco de Vitoria, Ctra, Pozuelo-Majadahonda 1800, Pozuelo de Alarcón, 28223 Madrid, Spain*
[b] *Departamento de Química, Universidad de las Islas Baleares, Cra. de Valldemossa km 7.5, 07122, Palma de Mallorca, Spain*
[c] *Departamento de Q. Inorgánica y Q. Técnica, Facultad de Ciencias, Universidad Nacional de Educación a Distancia, UNED, Avda. Esparta s/n, Ctra de Las Rozas al Escorial Km 5, Las Rozas, 28232, Madrid, Spain*

ARTICLE INFO

Keywords:
Amino-grafted silica
Heterogeneous catalysts
Chromene derivatives
Fine chemicals

ABSTRACT

Novel series of amino-grafted mesoporous silica materials applied to the green and efficient synthesis of 2-amino-4*H*-chromenes, from salicylaldehydes and ethyl cyanoacetate, under mild and free-solvent conditions, is herein reported for the first time. These catalysts are easily prepared by using the post-synthetic method, by functionalizing the SBA-15 silica with the corresponding amino silanes. The observed catalytic performance is mainly controlled by the type and concentration of basic sites. The methodology herein reported could be considered as an environmentally friendly alternative for the selective chromene synthesis, which allows to achieve high yields in short reaction times using notably small amounts of the catalysts. The experimental results are also supported with theoretical calculations, which suggest that the amine groups at the silica surface are behind the observed catalytic performance with the assistance of the silica matrix.

1. Introduction

Mesoporous silicas are versatile materials which find application in a great variety of research domains, including from catalysis to nanomedicine, among others [1–4]. In past decades, the use of mesoporous silica for catalytic applications has exponentially grown, emphasizing on the periodic mesoporous silicas. Since this type of materials are easily prepared and functionalized, including multifunctional surface modifications, exhibit high thermal and chemical stability and their large surface area and well-sized and well-distributed pores, they can be considered as an alternative for the transformation of complex and bulky substrates. Their industrial applications include petroleum refining, petrochemical production [5] and obtaining numerous products of fine chemistry [6,7]. In more recent times, ordered mesoporous silica-based catalysts have acquired importance in carbon dioxide conversion to chemicals, such as cyclic and dialkyl carbonates, acyclic carbamates, carboxylic acids, methanol, methane and fuels, as an alternative to reduce CO_2 emissions [8].

On the other hand, chromene derivatives are considered versatile and biologically active scaffolds exhibiting antiviral, antiproliferative, antioxidant and antihistaminic effects, among others, but also promising compounds in schizophrenia and Alzheimer's treatment [9–12].

The traditional homogeneous catalysts reported for the synthesis of chromene derivatives, and specifically for 2-amino-4*H*-chromenes, are highly polluting organic amines [13], whereas molecular sieves [14], anion exchange resins, such as Amberlyst A-21 [15], doped hydrotalcites [16], and zirconium phosphate [17] have been used as heterogeneous catalysts. Other efficient alternatives comprise the use of ionic liquids, such as imidazolium sulfonates [18], bifunctional mesoporous metallosilicates [19,20], and more recently, amino-grafted metal--organic frameworks catalysts with basic properties [21], CaO-carbon materials obtained from PET and natural limestone [22], mesoporous hydrotalcite/SBA-15 [23] and hydrotalcite/hydroxyapatite composites [24]. The reported methodologies are characterized by the use of smaller catalyst amounts operating in absence of any solvent, under mild reaction conditions, and in some cases after notably short reaction times, affording the corresponding chromene derivatives in good to excellent conversions.

These studies have demonstrated that it is possible to simplify the complex isolation and purification methods, reducing the generation of

* Corresponding authors.
E-mail addresses: g.turnes@uib.es (G. Turnes-Palomino), eperez@ccia.uned.es (E. Pérez-Mayoral).

https://doi.org/10.1016/j.cattod.2024.114515
Received 8 November 2023; Received in revised form 22 December 2023; Accepted 8 January 2024
Available online 11 January 2024

contaminant effluents and, at the same time, decreasing the reaction times, thus lowering energy consumption. In this context, the goal of this work is the development of a family of amino-grafted SBA-15 mesoporous silicas, able to promote the green and efficient synthesis of 2-amino-4*H*-chromene derivatives, from salycilaldehydes and ethyl cyanoacetate, under mild and solvent-free conditions. These materials are easily prepared by post-synthetic functionalization of SBA-15 with the corresponding silane including amines of different nature, demonstrating that the reaction is mainly controlled by the type and concentration of basic catalytic sites.

2. Materials and methods

The materials used in this research were commercially available. Chemical reagents and solvents were purchased from Sigma-Aldrich, Alfa-Aesar or Carlo Erba.

2.1. Synthesis and characterization of mesoporous materials

Mesoporous SBA-15 silica was prepared following the experimental protocol proposed by Zhao et al. [25,26]. Briefly, 30 mL of deionized water and 4 g of Pluronic P123 (Sigma-Aldrich, ≥99.99%) were added to a 120 g of HCl solution (2 M). The mixture was stirred until a homogeneous solution was obtained. Then, it was heated until 313 K and tetraethyl ortosilicate (TEOS; Sigma-Aldrich >99%) was added. After that, the mixture was kept stirring during 24 h. Subsequently, the solution was introduced into a Teflon autoclave at constant pressure and 373 K during 48 h, under static conditions. The obtained material was filtered off, washed with water until neutral pH and dried at room temperature. Finally, the solid was calcined at 823 K for 6 h by setting the heating rate at 1 $K{\cdot}min^{-1}$.

Amino-grafted SBA-15 was functionalized by following the reported methodology by Lopez-Sanz et al. [27]. To sum up, an excess amount of the corresponding silane (6.65 mmol) was added to a suspension of dried 2 g of SBA-15 in 35 mL of toluene (Carlo Erba, 99.8%). The mixture was stirred during 5 h at room temperature. Then, the material was filtered off and washed with 20 mL of toluene in order to extract the unreacted silane. Finally, the solid was dried in vacuum at room temperature.

Selected silanes to carry out the grafting process were (3-aminopropyl)triethoxysilane (APTES; Sigma-Aldrich 99%), 3-(diethylamino) propyl]trimethoxysilane (DEAPTMS; Alfa Aesar, 98%), (3-methylaminopropyl)trimethoxysilane (MAPTMS; Alfa Aesar, 98%) and (3-(2-aminoethylamino)propyl)trimethoxysilane (2APTMS; Sigma-Aldrich 99%) obtaining the corresponding catalysts denoted as APTES/SBA-15, DEAPTMS/SBA-15, MAPTMS/SBA-15 and 2APTMS/SBA-15, respectively. This type of catalysts has been previously investigated in our research group and tested in the synthesis of coumarins [28].

Textural parameters of the materials were determined from N_2 adsorption/desorption isotherms obtained with an ASAP 2020 Surface Area and Porosity analyzer (Micromeritics). Amino-grafted SBA-15 samples were previously outgassed, before carrying out the measurements, at 353 K under high vacuum, overnight. After degasification process, the adsorption process was carried out with N_2 at 77 K. The isotherms data were analysed by using the BET method to determine the specific surface area and the two-dimensional nonlocal density functional theory (2D-NLDFT) model for the determination of pore volume and pore size distribution. The Dubinin-Radushkevich method was used to obtain the micropore volume (V_{micro}) from the adsorption branches of the measured isotherms. Total pore volume (V_T) was determined from the nitrogen amount adsorbed at relative pressure P/P_0 of 0.95. The difference between these volumes corresponds to the mesopore volume (V_{meso}). Broekhoff and de Boer method was followed to determine windows parameters.

XRD measurements were performed with use of a X'Pert Pro PANalytical's X-ray diffractometer using Cu Kα radiation (λ = 1.5406 Å, 45 kV, 40 mA), working within 2θ range of 4–90°, 0.005° of scan step size and 20 s of dwell time.

Fourier transform infrared spectra were determined using a Bruker Vertex 80V spectrometer, equipped with an MCT cryodetector. For IR experiments, thin self-supported wafers were prepared and outgassed under dynamic vacuum at 403 K during 8 h. The spectra were obtained at room temperature, with a resolution of 4 cm^{-1} and the number of the scans fixed in 64.

The mass changes accompanying the material synthesis were investigated by thermogravimetric analysis using a STD Q600 thermobalance, by heating 45 mg of each sample from room temperature to 1223 K in an inert helium atmosphere. The heating rate and gas flow were set at 10 $K{\cdot}min^{-1}$ and 100 $cm^3{\cdot}min^{-1}$, respectively.

2.2. Catalytic performance

In a typical experiment, 25 mg of catalyst was added to a mixture of salycilaldehyde **2** (2 mmol) and ethyl cyanoacetate **3** (4 mmol; Alfa-Aesar, > 98%) and the reaction mixture was stirred during 3 h at 323 K. The reactions were carried out in the multiexperiment work station Starfish, in a liquid phase, under atmospheric pressure and solvent-free conditions. Samples of the reacting mixtures were periodically taken, at 15, 30, 60, 120 and 180 min, for analysis by ^{1}H NMR. The samples were diluted with CH_2Cl_2 (1 mL; Sigma-Aldrich, >99.8%) and the catalyst was filtered off using a glass syringe equipped with a microfilter (Milipore, 0.45 μm HV). Finally, the solvent was evaporated under vacuum.

The used salycilaldehydes are 2-hydroxybenzaldehyde (Alfa-Aesar, 99%), 5-bromo-2-hydroxybenzaldehyde (Alfa-Aesar, 98%), 2-hydroxy-5-methoxybenzaldehyde (Alfa-Aesar, 98%) and 2-hydroxy-5-nitrobenzaldehyde (Alfa-Aesar, 98%).

The progress of the reactions was qualitatively monitored by thin layer chromatography (TLC) performed on a DC-Aulofolien/Kieselgel 60 F_{245} (Merck), using CH_2Cl_2/EtOH (98:2) mixture as an eluent.

The yield (or conversion) of the process is defined as the fraction of reactant **2** transformed at each reaction time into compounds **1a** and **1b**, determined by ^{1}H NMR.

Reaction products were characterized by ^{1}H NMR spectroscopy. Solution NMR spectra were recorded on a Bruker DRX 400 (9.4 Tesla, 400.13 MHz for 1 H) spectrometer with a 5-mm inverse-detection H-X probe equipped with a z-gradient coil, at 27 °C. Chemical shifts (δ in ppm) are given from internal solvent, $CDCl_3$ (Euriso-Top, 99.8%) 7.26 for ^{1}H.

TOF values were defined as TON values by considering a conversion lower than 50% of **2** when using a) **2/3** molar ratio = 2:4, b) **2/3** molar ratio = 4:8, and c) **2/3** molar ratio = 6:1, in the presence of 25 mg of the corresponding catalyst, at 303 K, under solvent-free conditions.

$$TON = Conversion \quad x \quad substrate \quad \mathbf{2}{\cdot}(mmol)/N \quad loading(mmol)$$

$$TOF = TON/t(h)$$

2.3. Computational studies

The calculations showed in this work were performed by using the Gaussian 09 software package [29], in gas phase, at 298 K. In order to optimize geometries, B3LYP hybrid functional was used, in combination with 6–31 G(d,p) basis set, this functional being a methodology used to study nanostructures. Stationary points were characterized by analysing the harmonic vibrational frequency, and the transition structures (TS) were confirmed to be first-order saddle points. To represent the desired reaction coordinate, the imaginary frequency was inspected in all TS. For key transition states the intrinsic reaction coordinate (IRC) was followed to ensure it connects the reactants and products.

3. Results and discussion

3.1. Synthesis and characterization of the catalysts

The investigated materials were prepared by functionalization of SBA-15, previously synthetized, with the corresponding commercially available silane. As can be seen in Fig. 1a, XRD diffractograms for the SBA-15 matrix and amino-grafted materials showed well-resolved diffraction lines at low angles evidencing the hexagonal structure of the samples. All the materials also showed a type IVa isotherm accompanied by an H1 hysteresis loop (Fig. 1b). As expected, the synthesized SBA-15 matrix showed a predominantly mesoporous structure and high surface area (Table 1). After functionalization, micro- and mesoporosity are notably decreased in all the materials, probably due to a partial blockage of the pores by the incorporated functional groups, originating a pronounced diminution in surface area from 579 $m^2 \cdot g^{-1}$ to 269 $m^2 \cdot g^{-1}$ in the case of 2APTMS/SBA-15 sample. The pore diameter of the functionalized SBA-15 samples (between 64 and 49 Å) decreased compared with pristine SBA-15 (65 Å), being lower for the materials with higher N content (Table 1).

The results of the elemental analysis for amino functionalized samples confirm the presence of N (Table 1). As it can be seen, different concentrations of amine groups anchored to the silica surface were observed. The lower content for DEAPTMS/SBA-15 samples would be related to the presence of higher C% in the starting silane by the presence of ethyl groups. In the same context, the highest N loading for 2APTMS/SBA-15 catalyst is attributed to the presence of primary and secondary amine functions. It is surprising the low concentration of amine groups in MAPTMS/SBA-15 sample. This feature could be due to the interaction of basic amine function with silica matrix by hydrogen bonding inhibiting the grafting processes. These interactions for 2APTMS/SBA-15 and DEAPTMS/SBA-15 samples should be weak because of the presence of bulking substituents.

Samples under study were also investigated through FTIR spectroscopy (Fig. 2). For the samples APTES/SBA-15, DEAPTMS/SBA-15 and 2APTMS/SBA-15, the almost total disappearance of the band at 3745 cm^{-1}, assigned to isolated silanol groups, was observed [30], indicating a high functionalization degree (Fig. 2). However, the MAPTMS/SBA-15 sample showed a lower functionalization degree exhibiting an FTIR profile quite similar to SBA-15. All these results are in accordance with compositional data shown in Table 1. The broad adsorption band in the range of 3700–3250 cm^{-1}, assigned to the O-H stretching mode of hydrogen-bonded silanols [31], is present in all the explored samples, suggesting the presence of neighbouring silanols at the silica surface. In the case of the samples APTES/SBA-15 and MAPTMS/SBA-15, the bands corresponding to amine groups (1595 cm^{-1}) [32] indicate the formation of hydrogen bonds between amine functions and silanol groups acting as hydrogen acceptors and donors, respectively. For the 2APTMS/SBA-15 sample, additional bands, at 3362 and 3301 cm^{-1}, assigned to asymmetric and symmetric -NH_2 stretch hydrogen bonded amino group were observed as expected [33]. On the other hand, it was identified the presence of unreacted -OCH_3 groups as demonstrated by the presence of bands at 2973 and 2884 cm^{-1} corresponding to asymmetric and symmetric -CH_3 stretch [34].

Thermogravimetric analysis of the samples indicated that these materials are thermally stable from room temperature to approximately 473 K. In the case of SBA-15 matrix, it was observed a mass loss lower than 5% until 373 K, attributed to the removal of physically adsorbed water in pores. For amino-grafted samples, there is also a weight loss in the temperature range of 523–773 K because of the decomposition of organic moieties, confirming the functionalization of SBA-15 matrix.

3.2. Catalytic performance

The catalytic behaviour of the investigated materials was studied for the synthesis of 2-amino-4*H*-chromenes **1**, between 2-hydroxybenzaldehyde **2** and ethyl cyanoacetate **3**, under solvent-free conditions (Scheme 1). Based on previous studies and for comparison purposes, the reaction at 323 K was firstly carried out. All the catalysts led to the corresponding chromene derivatives with conversion values to **1** up to 87% in only 60 min of reaction time, except APTES/SBA-15 sample, which reached lower conversions at the shortest reaction times (Fig. 3a). Note that a pure sample of chromenes **1** was obtained in all cases after 3 h.

It is noteworthy that all the active catalysts provided diastereomeric mixtures of chromenes **1a/1b** in approximately 2:1 ratio, the major compound being the most thermodynamically stable isomer **1a**, as expected. Having in mind these results, the observed reactivity could be attributed to the basicity of the catalysts as an important factor to be considered. Taking into account the high conversion values to **1** in the presence of these amino-grafted SBA-15 mesoporous silicas, even at shortest reaction times, and in order to establish differences between catalysts, the catalytic behaviour was explored at a lower temperature, 303 K (Fig. 3b). In this case, all the catalysts were also active in the synthesis of chromenes **1**, giving the corresponding chromenes with lower conversions, as expected, but showing significant differences. As anticipated, by one side, it was observed that the conversion strongly depends on the basicity of the samples following the reactivity order: APTES/SBA-15 < MAPTMS/SBA-15 < 2APTMS/SBA-15 < DEAPTMS/SBA-15. In general, it is well-known that alkyl-substituted amines behave as stronger bases as their number of substituents increases, due to the inductive effects of alkyl groups on the nitrogen atom [35]. An

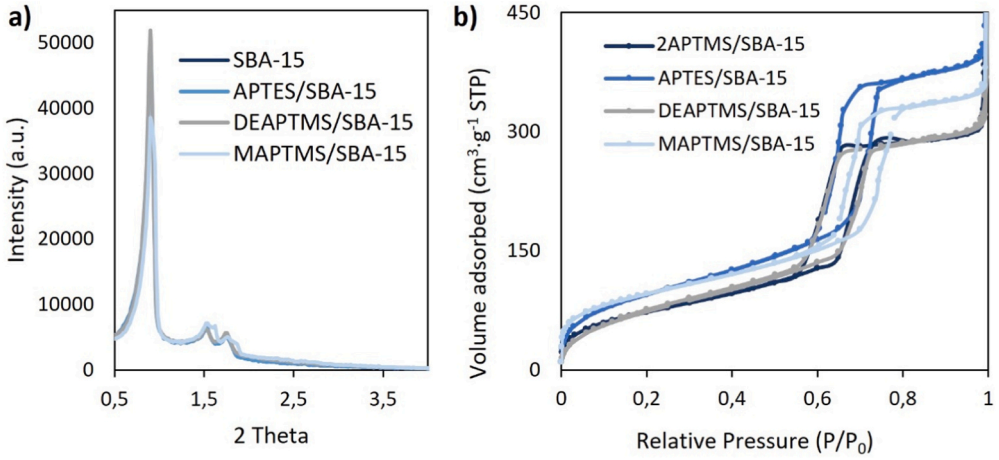

Fig. 1. a) XRD patterns for SBA-15 and amino-grafted SBA-15 catalysts. b) Adsorption/desorption isotherms of amino-grafted SBA-15 catalysts.

Table 1
Textural parameters and nitrogen loading in SBA-15 samples.

Catalyst	BET S_{BET} ($m^2 \cdot g^{-1}$)	($P/P_0 = 0.95$) V_T ($cm^3 \cdot g^{-1}$)	Dubinin-Radushkevich V_{micro} ($cm^3 \cdot g^{-1}$)	V_{meso} ($cm^3 \cdot g^{-1}$)	BdB D (Å)	N loading (mmol·g^{-1})[a]
SBA-15	579	0.97	0.04	0.93	65	-
APTES/SBA-15	332	0.63	0.00	0.63	60	2.19
DEAPTMS/SBA-15	271	0.50	0.00	0.50	55	1.72
MAPTMS/SBA-15	326	0.56	0.01	0.55	64	0.42
2APTMS/SBA-15	269	0.47	0.05	0.42	49	2.8

S_{BET}: BET surface, V_T: total pore volume, V_{micro}: microporous volume, V_{meso}: mesoporous volume, D (Å): diameter determined by Broekhoff and de Boer method.
[a] Determined by elemental analysis.

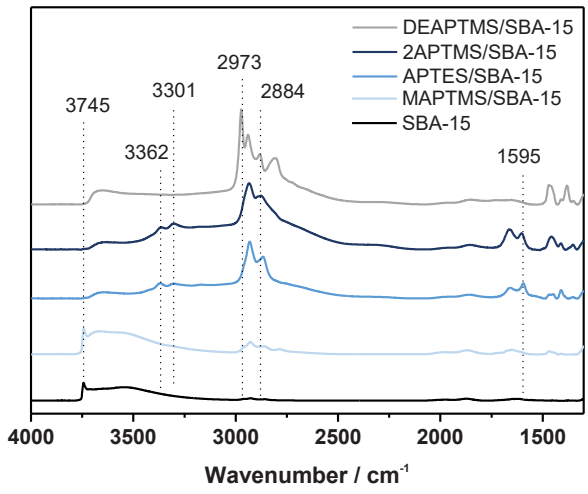

Fig. 2. FTIR spectra of SBA-15 and amino-grafted SBA-15 samples.

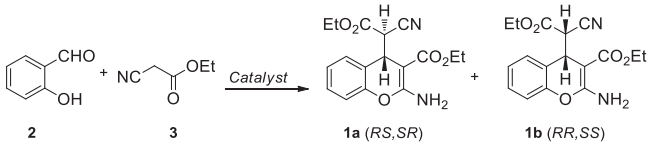

Scheme 1. Synthesis of 2-amino-4*H*-chromenes 1 from salicylaldehyde 2 and ethyl cyanoacetate 3 under solvent-free conditions.

example to be mentioned is the catalytic behaviour of MAPTMS/SBA-15 sample compared to APTES/SBA-15. In this case, it is observed a clear influence of basicity of the amine groups; while APTES/SBA-15 shows a considerably higher N content (2.19 *vs* 0.42 mmol·g^{-1}) and similar S_{BET} (~330 $m^2 \cdot g^{-1}$) and pore size distribution (Table 1), MAPTMS/SBA-15 exhibited an enhancement of the catalytic performance —45% of conversion *vs* 23% observed for APTES/SBA-15 after only 60 min—. Considering the SBA-15 grafted with secondary amines, MAPTMS/SBA-15 and 2APTMS/SBA-15 samples, and assuming that, although 2APTMS/SBA-15 contains primary and secondary amine groups and both functions should not simultaneously work, available -NH- functions in 2APTMS/SBA-15 are probably behind the enhanced conversion values observed. The same consideration in combination with the higher basicity of tertiary amine groups can be made for DEAPTMS/SBA-15. Regarding the texture parameters of the samples, it seems that porosity does not influence the catalytic performance probably because the pore sizes of the catalysts, in all the cases, are large enough to allow the appropriated diffusion of reactants and products. It is important to mention that SBA-15 sample was also tested resulting completely inactive by itself in the synthesis of chromenes **1**, even at the highest temperature (323 K), as expected. Therefore, SBA-15 mesoporous silica acts as a support of active phases, in our case, differently substituted amine functions.

In all the investigated cases, chromene **1a** was the major isomer, conversion to **1a** being in the range of 57–77% (at 303 K) or 69–81% (at 323 K) depending on the catalysts and the reaction temperature, in both cases after 3 h of reaction time (Fig. 4a). A slightly lower selectivity towards **1a** can be observed at 303 K, compared to that obtained at higher temperature, 323 K. The notable increase in selectivity (80%) in the presence of APTES/SBA-15 catalyst, at 323 K, could be attributed to epimerization of isomer **1b** to **1a** as previously observed when using other basic metallosilicates [20]. Although selectivity to **1a** increased

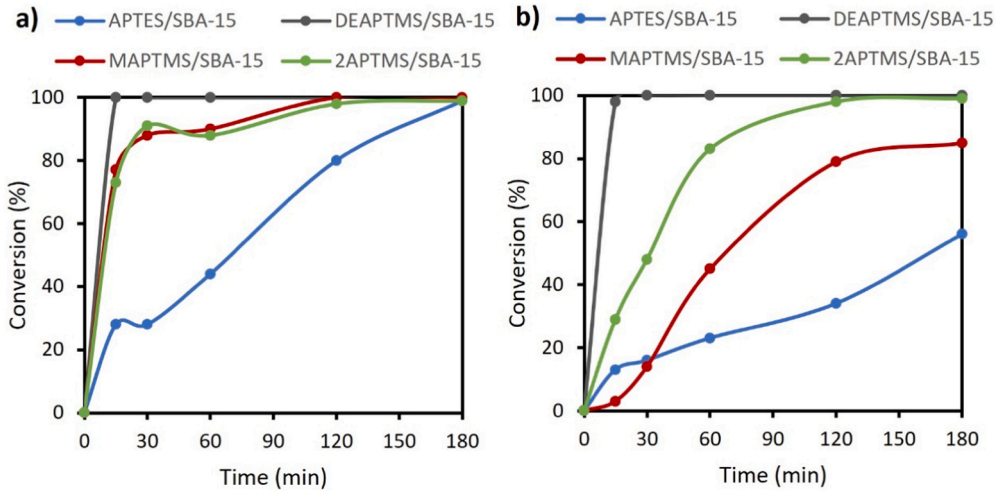

Fig. 3. Synthesis of 2-amino-4*H*-chromenes **1** promoted by amino-grafted/SBA-15 catalysts at a) 323 K and b) 303 K. Reaction conditions: 25 mg of the catalyst, **2**/**3** molar ratio = 2:4, solvent-free conditions.

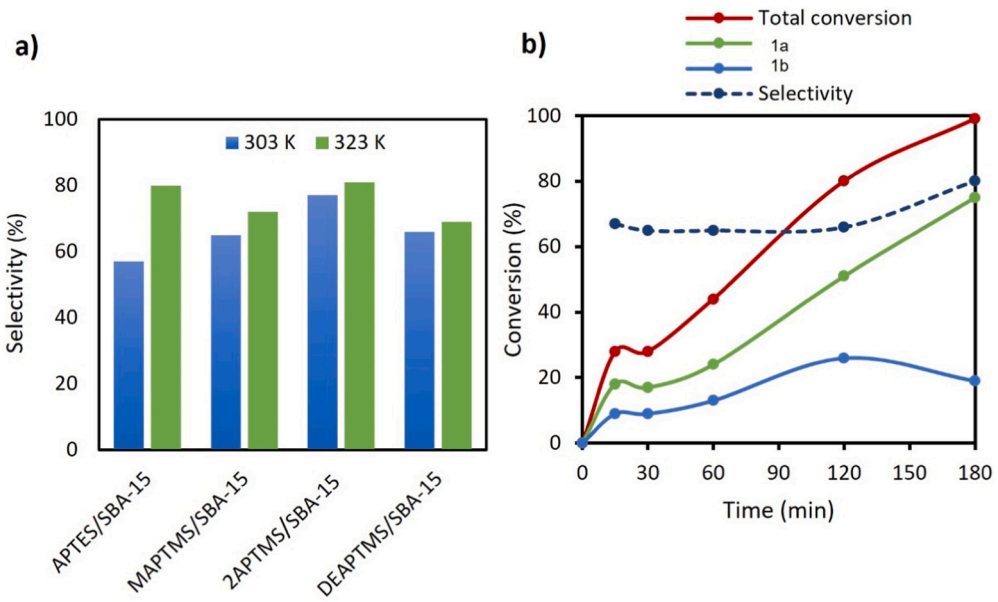

Fig. 4. Synthesis of chromenes **1** promoted by amino-grafted SBA-15 catalysts, a) selectivity to **1a** after 180 min of reaction time, at 323 and 303 K. b) Conversion values and selectivity variation to isomer **1a** using APTES/SBA-15 as catalyst at 323 K. Reaction conditions: 25 mg of catalysts, solvent-free conditions.

with the reaction time in all the investigated cases, this effect was considerably enhanced in the presence of APTES/SBA-15 catalyst, at 323 K (Fig. 4b). In this case, APTES/SBA-15 was the catalyst with the highest S_{BET} (332 $m^2 \cdot g^{-1}$) and V_{meso} (0.63 $cm^3 \cdot g^{-1}$), which probably allows the isomer interconversion (Table 1). The superior selectivity to **1a** (81% at 323 K) when using 2APTMS/SBA-15 (S_{BET} = 269 $m^2 \cdot g^{-1}$ and V_{meso} = 0.42 $cm^3 \cdot g^{-1}$) could be then due to some type of confinement effect. Thus, it seems that the diastereoselectivity to **1a** is depending on the texture of the samples, mainly the mesoporosity, in such a manner that high diastereoselectivity was observed when using the samples with lower V_{meso} values (Fig. 4b).

The influence of the catalyst amount in the reaction was also explored by modifying, in this case, the reactant molar ratio but maintaining the catalyst amount at 25 mg. Three experiments were carried out by increasing the reactant amounts (2-hydroxybenzaldehyde **2**/ethyl cyanoacetate **3** ratio (mmol)): a) **2**/**3** = 2:4, b) **2**/**3** = 4:8 and c) **2**/**3** = 6:12. Thus, the amount of the corresponding catalyst was reduced from 3.5% to 1.7% and 1.2% expressed in wt% regarding total reactant amounts. As it can be observed from Fig. 5, as expected, the conversion values decreased when increasing the reactant amounts, although most of the catalysts remain actives (Fig. 5). Remarkably, DEAPTMS/SBA-15 afforded chromenes **1** with quantitative conversion after 1 and 2 h when the reactant molar ratio was 4:8, and 6:12, respectively. However, APTES/SBA-15 catalyst was found to be almost inactive when the reactant amount was increased.

In order to evaluate the extension of the silanes leaching, we achieved additional experiment consisting of the reaction of 2-hydroxybenzaldehyde **2** and ethyl cyanoacetate **3** (**2**/**3** molar ratio = 4:8) in the presence of the most active catalyst, DEAPTMS/SBA-15 (25 mg), at 303 K, in such a manner that the catalyst was removed from the reaction mixture after 5 min of reaction time. Subsequently, the mixture was maintained at 303 K after 60 min of reaction time. Under these conditions, chromenes **1** were obtained in at least 18% of conversion as mixture of chromenes **1a**/**1b** with maintained selectivity (2:1 ratio), confirming that no leaching of silane is produced. We also carried out reutilization experiments in the presence 2APTMS/SBA-15 catalyst (25 mg), at 323 K, using a 2/3 molar ratio of 2:4, observing a decrease of the conversion values (from 99% to 38%) with maintained selectivity

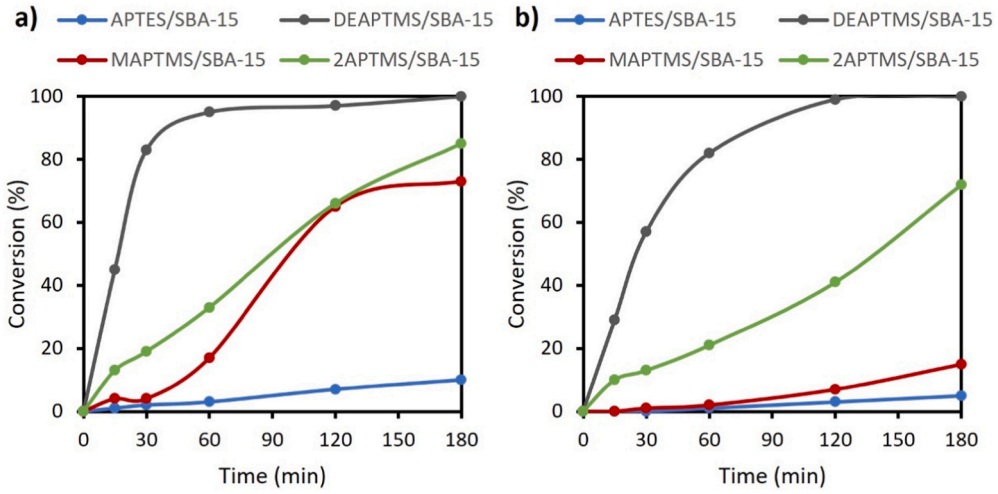

Fig. 5. Influence of catalyst amount in the synthesis of chromenes **1** catalysed by amino-grafted SBA-15 materials: a) **2**/**3** molar ratio = 4:8, b) **2**/**3** molar ratio = 6:12. Reaction conditions: 25 mg of catalysts, 303 K, solvent-free conditions.

during the second cycle, probably attributed to the strong interactions between functional groups in chromenes **1**, particularly cyano groups, and silanols (see computational section). This result is in accordance with those previously reported for amino-grafted metal-organic frameworks catalysts [21].

In addition, we also compare the catalytic activity of the investigated samples from the turnover frequency (TOF) values calculated, under different reaction conditions, only considering N loading, since amine functions are involved at least in the rate-limiting step, the aldol reaction between reagents (Table 2). DEAPTMS/SBA-15 highlights by its excellent catalytic activity, exhibiting the highest TOF values notably superior to those obtained for the other catalysts, but also decreasing when increasing the molar ratio of the reagents, as expected. The catalytic activity varies as follows: DEAPTMS/SBA-15 > MAPTMS/SBA-15 > 2APTMS/SBA-15 > APTES/SBA-15. Note the TOF decrease observed for MAPTMS/SBA-15 catalyst regarding to 2APTMS/SBA-15 when using a **2**/**3** molar ratio of 6:12, probably caused by the saturation of the catalytic sites, as shown in Fig. 5b.

Finally, the scope of the reaction was investigated from differently 5-substituted-2-hydroxybenzaldehydes **4** (Scheme 2) in the presence of the most efficient catalyst, DEAPTMS/SBA-15, under the same reaction conditions, at 303 K.

In this case, the observed reactivity order was H > Br > OMe > NO_2 (Fig. 6). The obtained results show that the substituted chromenes **5** can be easily synthesized with conversion values from good to excellent (up 95% after 1 h). Interestingly, the methodology herein reported constitutes a highly efficient alternative for the synthesis of ethyl 2-amino-6-bromo-4-(1-cyano-2-ethoxy-2-oxoethyl)− 4*H*-chromene-3-carboxylate **5** (**HA 14–1**), where R^1 is Br, in 98% of conversion and 70% of selectivity to **5a**, as a potential drug to be used in cancer treatment [11,36].

It is noteworthy that the presence of substituents on the aromatic ring of **4** modifies the acidity of the -OH group but also the electrophilicity of the -CHO function, influencing the reactivity. In is in accordance with previous studies concerning the synthesis of coumarins from salicylaldehydes substituted at 5-position and ethyl acetoacetate catalyzed by amino-grafted SBA-15 materials [28]. Both experimental and theoretical results indicated that the substituents do not interact with the corresponding catalyst, suggesting that the effect on the observed reactivity is electronic in nature, as expected. Substitution on aromatic ring modifies both electrophilicity of the carbonyl function but also on the acidity of the phenol depending on the substituent type. While strong electro-withdrawing substituent, in this case the NO_2 group, increased the acidy of the -OH group, the presence of electro-donor -OMe group increased the electrophilicity of the carbonyl acceptor in such a manner that the reaction proceeded with lower free-energy barrier when using salicylaldehydes bearing electro-donor substituents. This same trend has been also observed for the synthesis of chromene derivatives **5** investigated herein. In summary, the presence of -OMe and -Br substituents does not significatively affect the conversion values with respect to the unsubstituted 2-hydroxybenzaldehyde **2**, while the presence of the nitro group at the 5-position hindered the reaction leading to chromenes **5** with diminished conversion (37% and 97% after 1 and 3 h, respectively) (Fig. 6).

Table 2
TOF values for the investigated catalysts when working under different reaction conditions.

Catalyst	TOF (h^{-1})[a]	TOF (h^{-1})[b]	TOF (h^{-1})[c]
APTES/SBA-15	621	244	164
DEAPTMS/SBA-15	22326	16744	16186
MAPTMS/SBA-15	8571	6476	2000
2APTMS/SBA-15	5486	3771	3600

Reaction conditions: **2**/**3** molar ratio a) 2:4, b) 4:8 and c) 6:12, catalyst (25 mg), 303 K, solvent-free conditions.

3.3. Computational Study

In order to rationalize the obtained experimental results and based on previous studies concerning the mechanistic considerations in the synthesis of 2-amino-4*H*-chromenes [18], some theoretical calculations were made. Considering the first step as the rate-limiting one, the aldol condensation between reagents was studied. In this context, two different approaches were followed, involving i) only the basic centers of the catalysts comprising the amine functions, then acting as individual catalytic sites, but also ii) analysing the influence of the mesoporous silica as catalyst support, without considering the confinement restrictions if any. With this aim, considering the first approach, the reduced models shown in Fig. 7 were selected to study the catalytic behaviour of amine functions – primary, secondary and tertiary amines–.

The initial step of the reaction is the rate-determining step due to its reliance on the presence of bases. The amine function plays a crucial role in activating the nucleophile by abstracting the acidic proton in ethyl cyanoacetate **3**. Based on that, different potential interactions between the reactants and catalysts were explored, the most likely interactions illustrated in Fig. 7b. Specifically, for APTMS and MAPTMS catalysts, the spontaneous formation of the respective initial reactant complexes (RC) (Fig. 7b) were observed, each with free energy barrier values of − 4.8 and − 6.7 Kcal/mol, respectively, thus favouring the approach of the reactants. In the case of RC_{MAPTMS} (R^2 = Me), nearly all acidic protons in **3** were transferred to the amine function, confirming the major basic character of MAPTMS compared to APTMS. Consequently, a series of H-migrations occurred from ethyl cyanoacetate **3**, existing in its enol form, to the amine function, facilitating the activation of the electrophile—in this scenario, 2-hydroxybenzaldehyde **2**— *via* protonation of the -CHO group. Simultaneously, ethyl cyanoacetate **3** interacted with the -OH group in 2-hydroxybenzaldehyde **2** through hydrogen bonding. Note that this possibility is not viable in the case of DEAPTMS. This feature was already reported in our previous studies when investigating the amino-grafted SBA-15 materials as dual acid–base catalysts involved in the synthesis of coumarin derivatives from ethyl acetoacetate [28].

The preliminary inspection of the optimized transition state (TS) for the aldolization reaction catalyzed by amines revealed an increment of the H···O=CH distances depending on the specific nature of the amine (Fig. 8). The marked basic character of the amine functions on MAPTMS and DEAPTMS samples was consistent with larger H···O=CH distances—1.4222 and 1.4981 Å, respectively—compared to 1.3727 Å for TS_{APTMS}. However, the most advanced TS was TS_{MAPTMS} which presented the shortest C-C bond distance (2.0606 Å). The variation of C-C bond distances in TSs followed a similar trend than that observed for free-energy values ($TS_{DEAPTMS}$ > TS_{APTMS} > TS_{MAPTMS}) (Fig. 9a), suggesting that the MAPTMS catalyst should exhibit the best catalytic performance. In addition, we also computed the TS when using diethyl amine as catalyst. The $TS_{DIETHYLAMINE}$ was quite similar to TS_{MAPTMS} (C-C distance of 2.0442 Å) although showing a superior free-energy barrier up to 3.4 Kcal/mol compared to TS_{MAPTMS}. On the other hand, the highest free-energy barrier was observed for $TS_{DEAPTMS}$, 10.5 Kcal/mol higher than that observed for TS_{MAPTMS} probably attributed to steric effects. These results are in contrast with the observed catalytic performance for the sample functionalized with tertiary amine, DEAPTMS/SBA-15, which exhibited the best conversion to products after shortest reaction times. This circumstance could be firstly due to the high concentration of basic catalytic sites as confirmed by N loading determined by elemental analysis (Table 1).

We also studied the effect of the possible involvement of the silica matrix in the reaction. With this aim, we select the structural unit shown in Fig. 10 as the most suitable model cluster of SBA-15 molecular sieve [37]. Firstly, we studied the possible interactions of ethyl cyanoacetate **3** with the silica cluster. Calculations of the free-energy values when the cyano group in **3** interacts with the selected silica model, forming hydrogen bonds with the free-hydrogen of silanol, indicated a reduction

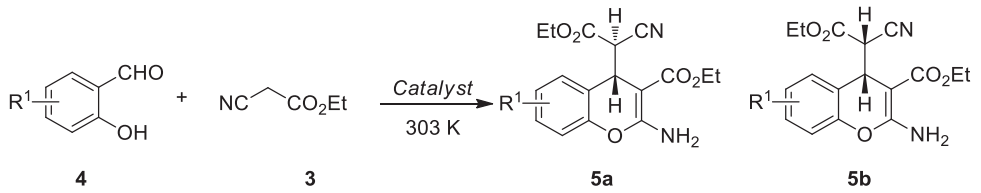

Scheme 2. Synthesis of 2-amino-4 H-chromenes **5** from different 5-substituted-2-hydroxy-aldehydes **4** and **3**, at 303 K, under solvent-free conditions.

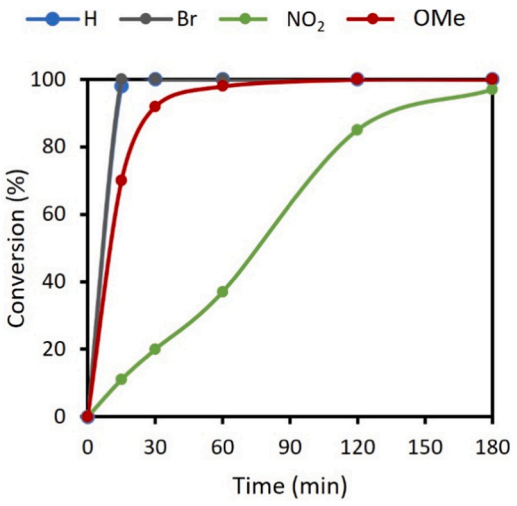

Fig. 6. Synthesis of 4*H*-chromenes **5** by using different 5-substituted-2-hydroxy-aldehydes **4** and ethyl cyanoacetate **3**, catalysed by DEAPTMS/SBA-15. Reaction conditions: 25 mg of catalysts, 303 K, **4**/**3** molar ratio = 2:4, solvent-free conditions.

of 3.0 to 3.6 kcal/mol compared to O- or C=O interactions. Taking these findings into consideration, the optimized TS depicted in Fig. 10b-c were found, maintaining the initial structures suggested earlier (Fig. 8). Here, the amine functions play a pivotal role in the activation of both nucleophile **3** and electrophile **2**, while the silica cluster is also engaged, holding both species through robust hydrogen bonding interactions – the cyano group in **3** with silanol (-C≡N···H-O-Si≡) and the phenolic hydrogen in **2** with basic centers (O-H···O≡Si) – . Considering the spontaneous formation of $RC_{MAPTMS\text{-}SBA}$, the free-energy barrier of both, $TS_{MAPTMS\text{-}SBA}$ and $TS_{DEAPTMS\text{-}SBA}$, just differs by 1.7 Kcal/mol less for $TS_{MAPTMS\text{-}SBA}$, but also the $TS_{DEAPTMS\text{-}SBA}$ is a more advanced transition state, as deduced from the C-C distance 2.1094 Å *vs* 2.3020 Å computed for $TS_{MAPTMS\text{-}SBA}$, being these results in accordance with the experimental results. Remarkably, the silica involvement notably reduces the free-energy values from 20.8 Kcal/mol (Fig. 9a) to 15 Kcal/mol for $TS_{DEAPTMS}$ and $TS_{DEAPTMS\text{-}SBA}$, respectively. Similar energy differences were also observed for $TS_{MAPTMS\text{-}SBA}$. Considering this scenario, it seems that the most probable TS for the aldolization of **2** with **3** is that in which amine functions are behind the observed reactivity but with assistance of the silica matrix allowing the reactant approach, more accused in the case of $TS_{DEAPTMS}$. Based on both experimental and theoretical results, amino-grafted mesoporous silicas can be considered as interesting and more sustainable alternative catalysts, particularly DEAPTMS/SBA-15 sample with a high concentration of active catalytic sites.

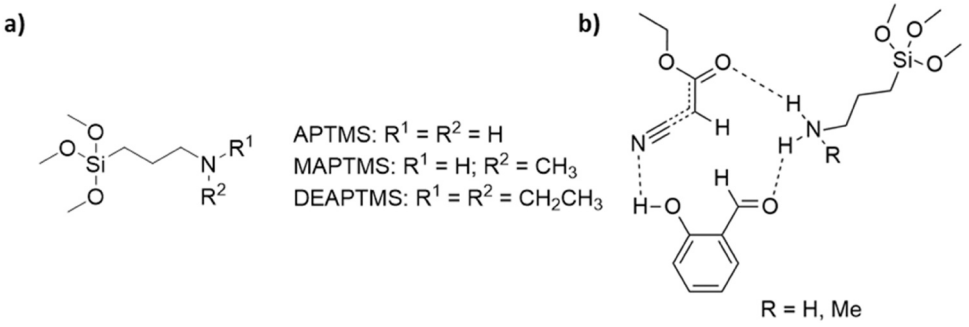

Fig. 7. a) Reduced models of amine-based catalysts. b) Reactant complexes indicating the reactants-amine interactions.

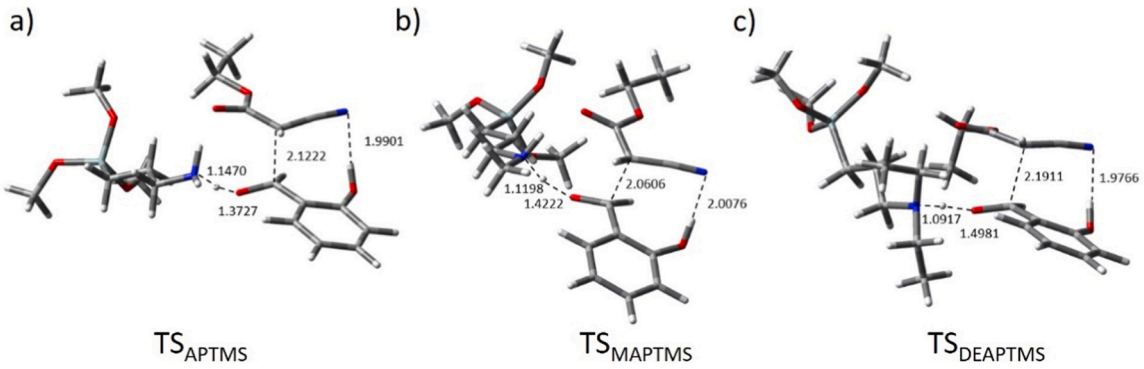

Fig. 8. Optimized TS for the aldol reaction between 2-hydroxybenzaldehyde **2** and ethyl cyanoacetate **3** catalyzed by amino-grafted mesoporous silicas when amine function acting as individual catalytic sites: a) TS_{APTMS}, b) TS_{MAPTMS}, and c) $TS_{DEAPTMS}$. Relevant distances are expressed in Å.

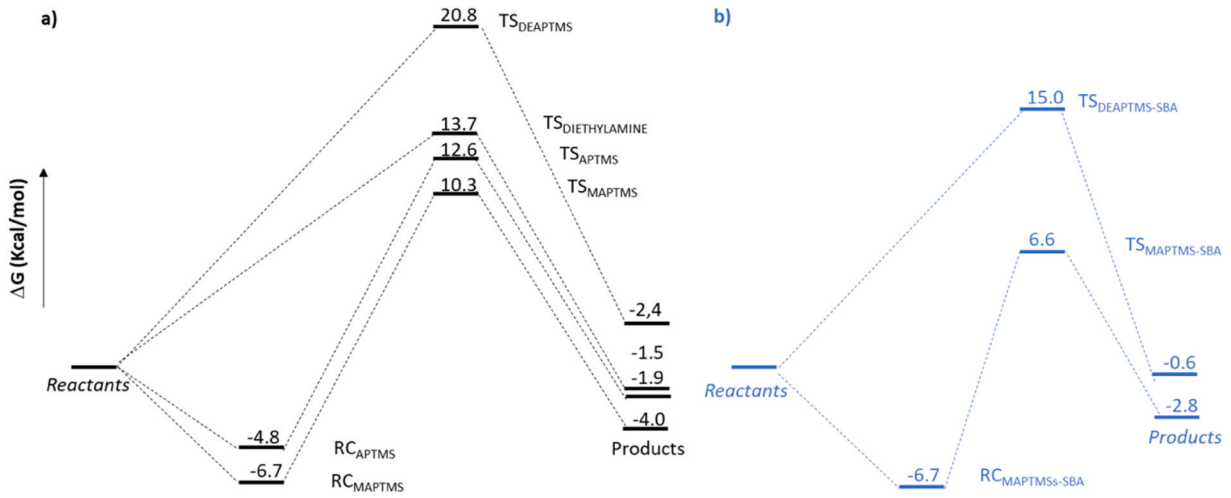

Fig. 9. Free-energy profiles for the aldolization reaction between 2-hydroxybenzaldehyde **2** and ethyl cyanoacetate **3** catalyzed by amino-grafted mesoporous silicas. a) Amines as individual catalytic sites. b) Amines with the assistance of the silica matrix.

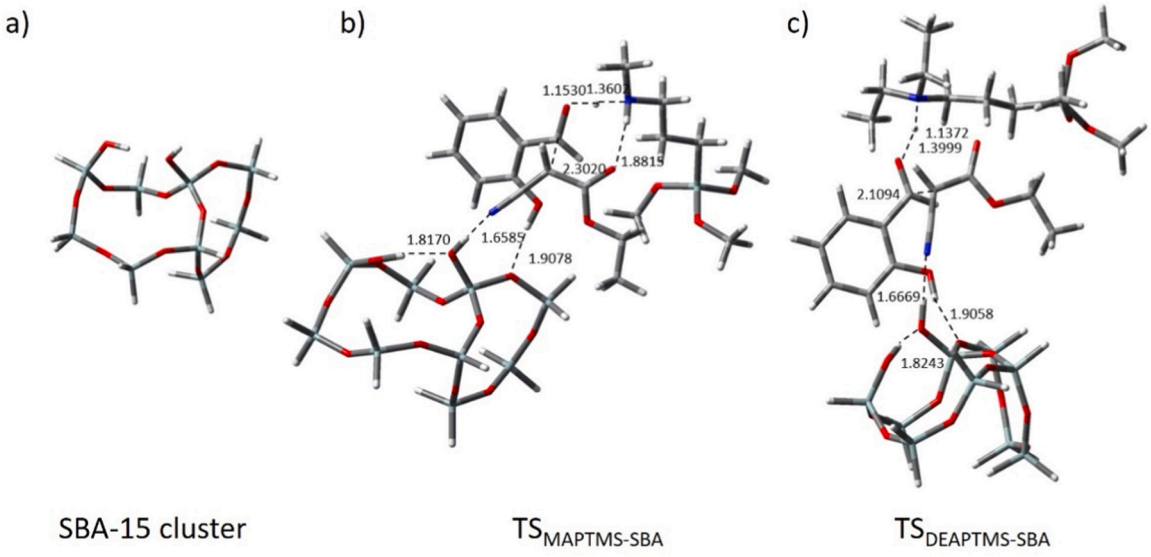

Fig. 10. Influence of catalytic support. Optimized TS for the aldol reaction between 2-hydroxybenzaldehyde **2** and ethyl cyanoacetate **3** catalyzed by amino-grafted mesoporous silicas. a) Silica cluster, b) $TS_{MAPTMS\text{-}SBA}$, and c) $TS_{DEAPTMS\text{-}SBA}$. Relevant distances are expressed in Å.

4. Conclusions

We report herein, for the first time, a family of amino-grafted SBA-15 catalysts, useful in the eco-efficient synthesis of 2-amino-4*H*-chromenes **1** and **5**, from different substituted 2-hydroxybenzaldehydes and ethyl cyanoacetate, under solvent-free and mild conditions. The catalysts were easily prepared by a post-synthetic method (grafting), functionalising the silica support with the corresponding aminosilanes.

The experimental results suggest that the catalytic performance is mainly governed by the basicity of the catalyst although it is influenced by considering also the concentration of amine function at the silica surface. In this context, DEAPTMS/SBA-15 sample was found to be the most efficient catalyst, showing the highest concentration of basic sites.

The theoretical calculations supported the experimental results. Considering the first step of the reaction as the rate-limiting step since it requires the presence of bases, the amine function role is the activation of the nucleophile by abstracting the acidic proton in ethyl cyanoacetate **3**. It was found that the silica support probably is involved in the reaction reducing the free-energy values of the corresponding optimized TS. It suggests that the most probable TS for the aldolization step is that in which amine functions are behind the observed reactivity but with the assistance of the silica matrix allowing the reactant approach. All these results strongly indicate that the silica matrix acts not only as support of the basic catalytic species, in this case the amine functions, but also contributes to the stabilization of the suggested TS.

In summary, the amino-grafted SBA-15 catalysts reported, particularly DEAPTMS/SBA-15, emerge as eco-friendly catalysts alternative to other materials, showing notably catalytic performance affording the corresponding chromenes with almost quantitative conversion values even at shorter times and using less amount of catalyst.

CRediT authorship contribution statement

González-Rodal Daniel: Investigation Writting - original draft. **PEREZ-MAYORAL ELENA:** Conceptualization, Funding acquisition, Supervision, Writing – original draft, Writing – review & editing. **López-Peinado Antonio J.:** Investigation. **Palomino-Cabello Carlos:** Investigation. **Turnes-Palomino Gemma:** Supervision. **Godino-Ojer Marina:** Investigation, Funding acquisition.

Declaration of Competing Interest

The authors declare that they have no known competing financial interests or personal relationships that could have appeared to influence the work reported in this paper.

Data Availability

Data will be made available on request.

Acknowledgements

This work has been supported by MCIN/AEI/ 10.13039/ 501100011033 (Project ref. PID2021-126579OB-C32) and Universidad Francisco de Vitoria de Madrid (Project Ref. FV2023-38).

References

[1] Y. Wang, Q. Zhao, N. Han, L. Bai, J. Li, J. Liu, E. Che, L. Hu, Q. Zhang, T. Jiang, S. Wang, Mesoporous silica nanoparticles in drug delivery and biomedical applications, Nanomed.: NBM 11 (2015) 313–327.
[2] R. Schmid, N. Neffgen, M. Linden, Straightforward adsorption-based formulation of mesoporous silica nanoparticles for drug delivery applications, J. Colloid Interface Sci. 640 (2023) 961–974.
[3] V.C. Niculescu, Mesoporous silica nanoparticles for bio-applications, Front. Mater. Sci. 7 (2020) 95–108.
[4] X. Yu, C.T. Williams, Recent advances in the applications of mesoporous silica in heterogeneous catalysis, Catal. Sci. Technol. 12 (2022) 5765–5794.
[5] C. Martinez, A. Corma, Inorganic molecular sieves: Preparation, modification and industrial application in catalytic processes, Coord. Chem. Rev. 255 (2011) 1558–1580.
[6] E. Pérez Mayoral, E. Soriano, V. Calvino-Casilda, M.L. Rojas-Cervantes, R. M. Martin-Aranda, Silica-based nanocatalysts in the C-C and C-heteroatom bond forming cascade reactions for the synthesis of biologically active heterocyclic scaffolds, Catal. Today 285 (2017) 65–88.
[7] E. Pérez-Mayoral, M. Godino-Ojer, D. González-Rodal, Bifunctional porous catalysts in the synthesis of valuable products, in: V. Calvino-Casilda, J.A. López-Peinado, R.M. Martin-Aranda, E. Perez-Mayoral (Eds.), Nanocatalysis: Applications and Technologies, Taylor & Francis Group London, 2019, pp. 25–61.
[8] A. Velty, A. Corma, Advanced zeolite and ordered mesoporous silica-based catalysts for the conversion of CO_2 to chemicals and fuels, Chem. Soc. Rev. 52 (2023) 1773–1946.
[9] V. Raj, J. Lee, 2H/4H-chromenes-A versatile biologically attractive scaffold, Front. Chem. 8 (2020) 1–23.
[10] S.R. Kesten, T.G. Heffner, S.J. Johnson, T.A. Pugsley, J.L. Wright, L.D. Wise, Design, synthesis, and evaluation of chromen-2-ones as potent and selective human dopamine D4 antagonists, J. Med. Chem. 42 (1999) 3718–3725.
[11] H.K. Keerthy, M. Garg, C.D. Mohan, V. Madan, D. Kanojia, R. Shobith, S. Nanjundaswamy, D.J. Mason, A. Bender, Basappa, K.S. Rangappa, P. Koeffler, Synthesis and characterization of novel 2-amino-chromene-nitriles that target Bcl-2 in acute myeloid leukemia cell lines, PLoS One 9 (2014) 1–11.
[12] C. Brühlmann, F. Ooms, P.A. Carrupt, B. Testa, M. Catto, F. Leonetti, C. Altomare, A. Carotti, Coumarins derivatives as dual inhibitors of acetylcholinesterase and monoamine oxidase, J. Med. Chem. 44 (2001) 3195–3198.
[13] M.A. Kulkarni, K.S. Pandit, U.V. Desai, U.P. Lad, P.P. Wadgaonkar, Diethylamine: a smart organocatalyst in eco-safe and diastereoselective synthesis of medicinally privileged 2-amino-4H-chromenes at ambient temperature, C. R. Chim. 16 (2013) 689–695.
[14] N.F. Yu, J.M. Aramini, M.W. Germann, Z.W. Huang, Reactions of salicylaldehydes with alkyl cyanoacetates on the surface of solid catalysts: syntheses of *4H*-chromene derivatives, Tetrahedron Lett. 41 (2000) 6993–6996.
[15] J.S. Yadav, B.V.S. Reddy, M.K. Gupta, I. Prathap, S.K. Pandey, Amberlyst A-21®: An efficient, cost-effective and recyclable catalyst for the synthesis of substituted *4H*-chromenes, Catal. Commun. 8 (2007) 2208–2211.
[16] U. Costantino, M. Curini, F. Montanari, M. Nocchetti, O. Rosati, Hydrotalcite-like compounds as heterogeneous catalysts in liquid phase organic synthesis.: II.: Preparation of *4H*-chromenes promoted by hydrotalcite doped with hydrous tin (IV) oxide, Microporous Mesoporous Mater. 107 (2008) 16–22.
[17] M. Curini, F. Epifano, S. Chimichi, F. Montanari, M. Nocchetti, O. Rosati, Potassium exchanged layered zirconium phosphate as catalyst in the preparation of *4H*-chromenes, Tetrahedron Lett. 46 (2005) 3497–3499.
[18] J. Velasco, E. Perez-Mayoral, V. Calvino-Casilda, A.J. Lopez-Peinado, M. A. Banares, E. Soriano, Imidazolium Sulfonates as Environmental-Friendly Catalytic Systems for the Synthesis of Biologically Active 2-Amino-*4H*-chromenes: Mechanistic Insights, J. Phys. Chem. B 119 (2015) 12042–12049.
[19] A. Smuszkiewicz, J. Lopez-Sanz, I. Sobczak, M. Ziolek, R.M. Martin-Aranda, E. Soriano, E. Perez-Mayoral, Mesoporous niobiosilicate NbMCF modified with alkali metals in the synthesis of chromene derivatives, Catal. Today 277 (2016) 133–142.
[20] A. Smuszkiewicz, J. Lopez-Sanz, I. Sobczak, R.M. Martin-Aranda, M. Ziolek, E. Perez-Mayoral, Tantalum vs Niobium MCF nanocatalysts in the green synthesis of chromene derivatives, Catal. Today 325 (2019) 47–52.
[21] D. Gonzalez-Rodal, G.T. Palomino, C.P. Cabello, E. Perez-Mayoral, Amino-grafted Cu and Sc Metal-Organic Frameworks involved in the green synthesis of 2-amino-*4H*-chromenes. Mechanistic understanding, Microporous Mesoporous Mater. 323 (2021) 111232–111243.
[22] D. Gonzalez-Rodal, J. Przepiorski, A.J. Lopez Peinado, E. Perez-Mayoral, Basic-carbon nanocatalysts in the efficient synthesis of chromene derivatives. Valorization of both PET residues and mineral sources, Chem. Eng. J. 382 (2020) 122795–122804.
[23] F.D. Velazquez-Herrera, D. Gonzalez-Rodal, G. Fetter, E. Perez-Mayoral, Enhanced catalytic performance of highly mesoporous hydrotalcite/SBA-15 composites involved in chromene multicomponent synthesis, Microporous Mesoporous Mater. 309 (2020) 110569–110579.
[24] F.D. Velazquez-Herrera, D. Gonzalez-Rodal, G. Fetter, E. Perez-Mayoral, Towards highly efficient hydrotalcite/hydroxyapatite composites as novel catalysts involved in eco-synthesis of chromene derivatives, Appl. Clay Sci. 198 (2020) 105833–105840.
[25] D.Y. Zhao, J.Y. Sun, Q.Z. Li, G.D. Stucky, Morphological control of highly ordered mesoporous silica SBA-15, Chem. Mater. 12 (2000) 275–279.
[26] D.Y. Zhao, J.L. Feng, Q.S. Huo, N. Melosh, G.H. Fredrickson, B.F. Chmelka, G. D. Stucky, Triblock copolymer syntheses of mesoporous silica with periodic 50 to 300 angstrom pores, Science 279 (1998) 548–552.
[27] J. Lopez-Sanz, E. Perez-Mayoral, E. Soriano, M. Sturm, R. Maria Martin-Aranda, A. J. Lopez-Peinado, J. Cejka, New inorganic-organic hybrid materials based on SBA-15 molecular sieves involved in the quinolines synthesis, Catal. Today 187 (2012) 97–103.
[28] N. Aider, A. Smuszkiewicz, E. Perez-Mayoral, E. Soriano, R.M. Martin-Aranda, D. Halliche, S. Menad, Amino-grafted SBA-15 material as dual acid base catalyst for the synthesis of coumarin derivatives, Catal. Today 227 (2014) 215–222.
[29] G.W.T.M.J. Frisch, H.B. Schlegel, G.E. Scuseria, M.A. Robb, J.R. Cheeseman, G. Scalmani, V. Barone, B. Mennucci, G.A. Petersson, H. Nakatsuji, M. Caricato, X. Li, H.P. Hratchian, A.F. Izmaylov, J. Bloino, G. Zheng, J.L. Sonnenberg, M. Hada, M. Ehara, K. Toyota, R. Fukuda, J. Hasegawa, M. Ishida, T. Nakajima, Y. Honda, O. Kitao, H. Nakai, T. Vreven, J.A. Montgomery Jr., J.E. Peralta, F. Ogliaro, M. Bearpark, J.J. Heyd, E. Brothers, K.N. Kudin, V.N. Staroverov, R. Kobayashi, J. Normand, K. Raghavachari, A. Rendell, J.C. Burant, S.S. Iyengar, J. Tomasi, M. Cossi, N. Rega, J.M. Millam, M. Klene, J.E. Knox, J.B. Cross, V. Bakken, C. Adamo, J. Jaramillo, R. Gomperts, R.E. Stratmann, O. Yazyev, A.J. Austin, R. Cammi, C. Pomelli, J.W. Ochterski, R.L. Martin, K. Morokuma, V.G. Zakrzewski, G.A. Voth, P. Salvador, J.J. Dannenberg, S. Dapprich, A.D. Daniels, Ö. Farkas, J. B. Foresman, J.V. Ortiz, J. Cioslowski, D.J. Fox, Gaussian 09, Gaussian, Inc.,, Wallingford CT, 2009.
[30] N. Hiyoshi, K. Yogo, T. Yashima, Adsorption characteristics of carbon dioxide on organically functionalized SBA-15, Microporous Mesoporous Mater. 84 (2005) 357–365.
[31] G. Paul, G.E. Musso, E. Bottinelli, M. Cossi, L. Marchese, G. Berlier, Investigating the interaction of water vapour with aminopropyl groups on the surface of mesoporous silica nanoparticles, ChemPhysChem 18 (2017) 839–849.
[32] A. Danon, P.C. Stair, E. Weitz, FTIR study of CO_2 adsorption on amine-grafted SBA-15: elucidation of adsorbed species, J. Phys. Chem. C. 115 (2011) 11540–11549.
[33] G.E. Musso, E. Bottinelli, L. Celi, G. Magnacca, G. Berlier, Influence of surface functionalization on the hydrophilic character of mesoporous silica nanoparticles, Phys. Chem. Chem. Phys. 17 (2015) 13882–13894.
[34] L.D. White, C.P. Tripp, Reaction of (3-aminopropyl)dimethylethoxysilane with amine catalysts on silica surfaces, J. Colloid Interface Sci. 232 (2000) 400–407.
[35] R.J. Ouellette, J.D. Rawn, Amines and amides, in: R.J. Ouellette, J.D. Rawn (Eds.), Organic Chemistry Study Guide. Key Concepts, Problems, and Solutions, Elsevier, Amsterdam, 2015, pp. 465–494.
[36] J.L. Wang, D.X. Liu, Z.J. Zhang, S.M. Shan, X.B. Han, S.M. Srinivasula, C.M. Croce, E.S. Alnemri, Z.W. Huang, Structure-based discovery of an organic compound that binds Bcl-2 protein and induces apoptosis of tumor cells, Proc. Natl. Acad. Sci. USA 97 (2000) 7124–7129.
[37] Z. Wang, D. Wang, Z. Zhao, Y. Chen, J. Lan, A. DFT, study of the structural units in SBA-15 mesoporous molecular sieve, Comput. Theor. Chem. 963 (2011) 403–411.